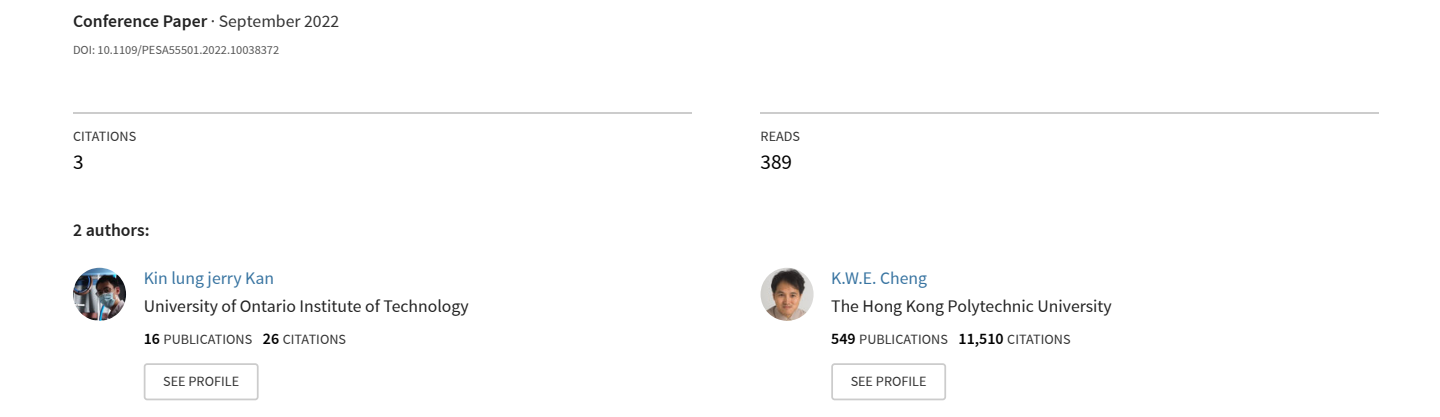
Review of Marine Magnetohydrodynamic Motor Development



Review of Marine Magnetohydrodynamic Motor Development

Kin Lung Jerry Kan¹, K.W.E. Cheng²

Power Electronics Research Centre, The Hong Kong Polytechnic University, Hong Kong ¹E-mail: jerry.kan@connect.polyu.hk, ²E-mail: eric-cheng.cheng@polyu.edu.hk.

Abstract— Magnetohydrodynamic motor applies the external electromagnetic field to the liquid inside the duct thereby generates the fluid flow without the propeller. The electric field accelerates the charged particles of the liquid whereas the magnetic field steers the direction. Rather than the vacuum analysis, it reacts in the fluid which introduces the analysis of Newtonian flow. Distribution of the electromagnetic field is another key feature. Simulations and prototypes of the former research would be presented and compared

Keywords— Electric vehicle, Magnetohydrodynamic motor, Marine electrification.

I. INTRODUCTION

Magnetohydrodynamic (MHD) motor accelerates the charged particles of the conductive liquid inside a hollow duct, by the excited Lorentz force from external magnetic and electric field. The force applied on the liquid pushes it from the inlet to the nozzle, abolishes the rotating mechanical propulsion system, such as propeller and the negative phenomenon: acoustic noise, cavitation, sealing of bearing and the harm to maritime creatures. A testing ship YAMATO-1 which is 30m in length was developed in 1996 illustrated the physic basics of the MHD propulsion and proved the practicability by the scale-down tests, and sea trials result [1]. Analysis of the propulsion Lorentz force is the main theory foundation of the topic [1-5]. The classical formula on the charged particle cannot suit the MHD application well, for the interactions from the molecule of liquid, such as Stoke's law, under the small Reynold's number fluid circumstances, rather than vacuum environment. The concept of Lorentz force density which is suitable to relate the fluid flow pressure analysis of the motor channel was presented in [6], to conduct velocity performances comparison of linear channel of MHD and that of helical. [7] also introduced it in the fluid Navier-Stoke (N-S) equations numerical model analysis, to predict the velocity profile of the arterial blood inside which the small swimming robot would be propelled by external magnetic field and electric wireless power transfer without mechanical contact part of the current.

Though that [8] exhibited a detailed magnetic equivalent circuit of MHD from the reluctance distribution circuit, the Finite Element Method (FEM) simulations reveals higher reliability for magnetic field estimation [9]. In this paper, the intuitive magnetic flux density has been processed by COMSOL and was depicted explicitly with figures, to evaluate the field distribution. The electric field, velocity speed of fluid and viscous stress could also be plotted in similar way. The overall computation simulation tree graph was revealed in [10].

A large 1:1 scale surface ship prototype YAMATO 1 was constructed and sailed for conceptual validation in 1992. She was long 3,000mm, had 1.50m design draft and 185tons displacement. There are 6pairs of MHD motors with superconducting magnetic field generation coil designed at maximum 4.0T magnetic flux at bore centre of 3,000mm effective magnetic field length and 175mm clearance of electrodes. Maximum 7.5kN speed was achieved at the 3.0T magnetic flux and 2000A electric conduction current in motor [1].

In section 2, the concepts and MHD applications development of the Lorentz force would be illustrated. The concept of force density would be explained so that the section 3, combination analysis of fluid dynamics and Lorentz force could be conducted smoothly. Simulation methods and the experimental detail could be found in section 4. Last section to summing the paper.

II. LORENTZ FORCE ANALYSIS

Though the Lorentz force is relatively correct, real relativistic transformation is ignored here, due to the very low-level fluid velocity of MHD motor propels when compared with the speed of light. It would be applied on the charged particle which moves in an electromagnetic field [11]. In Lorentz force law (1), p stands for the momentum vector of charged particle, of which the time derivative results in the force, react with the charge q, moving velocity v and external electromagnetic field parameter, electric field strength E, magnetic field density E. In MHD applications, the E directional component of E0 would be regarded as the current maintaining charge drift velocity, whereas that of the force contributes nothing to the fluid acceleration if their axes are orthogonal.

$$\frac{d\boldsymbol{p}}{dt} = q(\boldsymbol{E} + \boldsymbol{v} \times \boldsymbol{B}) \tag{1}$$

$$\boldsymbol{p} = m\boldsymbol{v} \tag{2}$$

And the kinetic energy ε could be estimated by the mass m and v in (3). After the derivative (4), we can find that on the charged particle, electric field does the work, meanwhile the force component of magnetic field F_{mag} that be normal to the velocity of charge, only changes the direction of velocity [12].

$$\frac{d\varepsilon}{dt} = v \cdot \frac{d\mathbf{p}}{dt} \tag{3}$$

$$\frac{d\varepsilon}{dt} = qv \cdot \mathbf{E} \tag{4}$$

$$\mathbf{F}_{mag} = q\mathbf{v} \times \mathbf{B} \tag{5}$$

In [6], the Lorentz force density of the magnetic component has been presented as (6) of which E stands for the fluid electric field strength, σ is the fluid electric conductivity.

$$f = \sigma(E - vB)B \tag{6}$$

III. INTEGRATION OF LORENTZ FORCE AND FLUID NAVIER-STOKES EQUATIONS

Fluid analysis features the force MHD motor from the other propeller based maritime thruster, as well as the jet thruster which contain the impeller inside. For the incompressible Newtonian flow, the second-order nonlinear partial differential Navier-Stokes (NS) equations with the numerical calculation methods, such as computational fluid dynamics (CFD) are effective to evaluate the velocity and pressure distributions of flow with the body forces and surface forces, such as the gravity, magnetism, electric potential and viscous effect respectively. It emphasizes the analysis of fluid flow into the performance of extremely small area or volume thereby the introducing of Lorentz force density at aforementioned section is necessary to be take use of [13]. Newtonian fluid represents the material that viscous stresses are proportional to the local strain rate of flow. [10] exhibited the combination of NS equations and magnetic component of Lorentz force as (7) in continuity, which indicates the flow obeying the conservation of mass at (8). The fluid flow velocity u is determined by the fluid density ρ , pressure of flow p_r , viscosity v_{is} ("Nu" rather than velocity "v" mentioned before), current density J and magnetic field density B. However, the electric component of Lorentz force is absence in these two formulas. The boundary condition of the flowing fluid is neither assigned.

$$\frac{du}{dt} = -\frac{1}{\rho} \nabla p_r + v_{is} \nabla^2 u + \frac{1}{\rho} j \times B$$

$$\nabla \cdot u = 0$$
(8)

The model developed by [14] improved the model by superposing the electric component of Lorentz force and applying the two parallel plates boundary condition of laminar flow. The fully developed NS equation estimated as (9), in which t is variable of time, f depicted as (6). Term x is flow directional axis, whereas y and z are directions of electric field and of B field

$$\rho \left(\frac{\partial u}{\partial t} + u \frac{\partial u}{\partial x} \right) = -\frac{dp_r}{dx} + \frac{\partial}{\partial x} \left(\mu \frac{\partial u}{\partial x} \right) + \frac{\partial}{\partial z} \left(\mu \frac{\partial u}{\partial z} \right) + f$$

$$(9)$$

A more intuitive model with 3-D estimation of flow velocity and the obtain of turbulent kinetic energy k were demonstrated [9]. Similarly, x axis representing the flowing direction, y axis and z axiz for direction of electric field strength and of magnetic field density. u, v, w here representing the velocity of x, y, z direction, viscous tensor

indicated as τ_{ij} that could be calculated by the k. and dissipation rate ε_d . Constant C_μ equals 0.09. The electric current density of the fluid was also illustrated in (14), the ohm's law for moving conductors raised in [15], even if the average velocity of charged particles stays at non-relativistic speed

$$\rho \left(u \frac{\partial u}{\partial x} + v \frac{\partial u}{\partial y} + w \frac{\partial u}{\partial z} \right)$$

$$= -\frac{dp_r}{dx} + \frac{\partial \tau_{xx}}{\partial x} + \frac{\partial \tau_{xy}}{\partial y} + \frac{\partial \tau_{xz}}{\partial z} + J_y B_z - J_z B_y$$
(10)

$$\rho \left(u \frac{\partial v}{\partial x} + v \frac{\partial v}{\partial y} + w \frac{\partial v}{\partial z} \right)$$

$$= -\frac{dp_r}{dx} + \frac{\partial \tau_{yx}}{\partial x} + \frac{\partial \tau_{yy}}{\partial y} + \frac{\partial \tau_{yz}}{\partial z} + J_z B_x - J_x B_z$$
(11)

$$\rho \left(u \frac{\partial w}{\partial x} + v \frac{\partial w}{\partial y} + w \frac{\partial w}{\partial z} \right)$$

$$= -\frac{dp_r}{dx} + \frac{\partial \tau_{zx}}{\partial x} + \frac{\partial \tau_{zy}}{\partial y} + \frac{\partial \tau_{zz}}{\partial z} + J_x B_y - J_y B_x$$
(12)

$$\tau_{ij} = (\frac{\rho C_{\mu} k^2}{\varepsilon} + \mu)(\frac{\partial u_i}{\partial x_i} + \frac{\partial u_j}{\partial x_i})$$
 (13)

$$J = \sigma[E + (v \times B)] \tag{14}$$

IV. SIMULATION AND EXPERIMENT METHOD

Numerical analysis and results comparison with the electric current, electric current density, MHD thruster-based vessel velocities with regarding the coil number-of-turn and width of thruster channel were plotted in [].

The overall design could be evaluated by the software COMSOL MultiPhysics which using the finite element method (FEM) to work out the enormous partial differential problems in space, time dependent and frequency dependent value. It comprises diverse study case upon different disciplines: Magnetic field, current, fluid including turbulent and laminar flow, plasma and so on. Properties of material such as conductivity, conductor cross-section area, viscosity, magnetic relative permeability and relative permittivity could be assigned in custom. Pressures along the MHD channel in [10], as well as the vector and value distribution of electric current density, of magnetic field and that of fluid velocity in channel were figured out [9]. Results of the 1750mm in length, 340mm in width and height, 2.2kA/m² current density, average 17T rectangular thruster generated the maximum 10.6m/s flow, consuming 226.357kW input power of magnetic field generation DC current and electric field maintaining current. the output power of thruster was 44.305kW, overall efficiency claimed at 20%. The scale-down experiment of it was formed as a 110mm in length, cross-section on 54*17mm² thruster with average 0.5T magnetic field and 3A conducting current. The conductivity of liquid was seawater liked, rated at 5.5S/m, enabled it flowed at the highest speed around 43cm/s in testing tube.

Experiments were conducted over the measurements of thrust force, pressure and velocity. (15) indicates the thrust force T estimation, with respect to density, flow in duct Q(m/s), jet stream velocity from nozzle U_n and the ship speed U_∞ . More than 6,000N thrust force was measured from the 12-thruster ship YAMATO 1 at condition of 1500A conducting current, 2T magnetic flux in each thruster. Thrust force combined with the calculation of Lorentz force, the relation of them showed as positive proportional. Another 900-lb displacement submarine, EMS-1 was built in 1966. A half hull 5-in channel installed and got the 0.4m/s sailing speed at 0.015T circumstance [2].

$$T = \rho Q(U_n - U_\infty) \tag{15}$$

V. CONCLUSION

This paper provides an insight into the recent development of the MHD thruster. The introduction of the sailing prototypes about the outline and dimensional parameters, field generation profiles of magnetic and electric field, analysis of Lorentz force and its interaction with fluid dynamics. Current density in thruster would increase with the incremental flowing speed from the ohm's law for moving conductor. Furthermore, the development of fluid analysis from open channel to parallel plain, from laminar flow to turbulence have enrich the application of MHD motor. Apart from numerical iterative calculations, the FEM simulation software provides a more intuitive and accurate demonstration of electrode and field generation design. Experimental testing was described in this paper, however, more prototypes are in desire to validate the solid theory about the fluid thrust force regarding the flow channel shape and material design, Lorentz force and impact of installation position.

ACKNOWLEDGMENT

The authors wish to acknowledge the support provided by the members of the Power Electronics Research Centre (PERC), Department of Electrical Engineering, The Hong Kong Polytechnic University.

REFERENCES

- Y. Sasakawa, S. Takezawa, Y. Sugawara, and Y. Kyotani, "The superconducting MHD-propelled ship YAMATO-1," 1995.
- [2] S. Way, "Electromagnetic Propulsion for Cargo Submarines," Journal of Hydronautics, Vol. 2, No. 2, pp.49-57.
- [3] S. Vader, "Advances in Magnetohydrodynamic Liquid Metal Jet Printing," TechConnect Briefs, vol. 4, pp. 41–45, 2016.
- [4] G. G. Branover and A. B. Tsynober Magnetic Hydrodynamics of Incompressible Environments. Moscow: Nauka, 1970.
- [5] E. D. Doss and H. K. Geyer, "MHD seawater propulsion", J. Ship Res., vol. 37, no. 1, pp. 49-57, 1993.
- [6] M. Haghparast and M. R. A. Pahlavani, "A Comparative Study on the Performance of Marine Magnetohydrodynamic Motors With Helical and Linear Channels," in IEEE Transactions on Magnetics, vol. 55, no. 11, pp. 1-8, Nov. 2019, Art no. 8205008, doi: 10.1109/TMAG.2019.2927703
- [7] T. S. Gregory et al., "Magnetohydrodynamic-Driven Design of Microscopic Endocapsules in MRI," in IEEE/ASME Transactions on Mechatronics, vol. 20, no. 6, pp. 2691-2698, Dec. 2015, doi: 10.1109/TMECH.2015.2412517.

- [8] I. A. Smolyanov, E. L. Shvydkiy, F. N. Sarapulov and S. F. Sarapulov, "Research electromechanical characteristics of magnetohydrodynamic pump," 2017 IEEE Conference of Russian Young Researchers in Electrical and Electronic Engineering (ElConRus), 2017, pp. 1590-1593, doi: 10.1109/ElConRus.2017.7910877.
- [9] M. Haghparast, M. R. Alizadeh Pahlavani and D. Azizi, "Fully 3-D Numerical Investigation of Phenomena Occurring in Marine Magnetohydrodynamic Thrusters," in IEEE Transactions on Plasma Science, vol. 47, no. 4, pp. 1818-1826, April 2019, doi: 10.1109/TPS.2019.2901305.
- [10] I. Martynovich, A. Avdeev and A. Drobotov, "Magnetohydrodynamic Pump Work Simulation," 2018 International Russian Automation Conference (RusAutoCon), 2018, pp. 1-5, doi: 10.1109/RUSAUTOCON.2018.8501760.
- [11] Anupam Garg, "Classical Electromagnetism in a Nutshell", 2012, pp.252.
- [12] Lerner, L. S. (1996). Physics for scientists and engineers. Jones and Bartlett.
- [13] F. M. White, Fluid mechanics, 7th ed. New York, N.Y: McGraw Hill,
- [14] M. Trapanese, F. M. Raimondi, D. Curto and A. Viola, "A computational magnetohydrodynamic model of a marine propulsion system," OCEANS 2016 - Shanghai, 2016, pp. 1-4, doi: 10.1109/OCEANSAP.2016.7485711.
- [15] P. Lorrain, F. Lorrain, and S. Houle, Magneto-Fluid Dynamics: Fundamentals and Case Studies of Natural Phenomena. New York, NY: Springer New York.